

Article

Study on Degradation of Natural Rubber Latex Using Hydrogen Peroxide and Sodium Nitrite in the Presence of Formic Acid

Kraiwut Wisetkhamchai ¹, Weerawat Patthaveekongka ¹ and Wanvimon Arayapranee ^{2,*}

¹ Department of Chemical Engineering, Faculty of Engineering and Industrial Technology, Silpakorn University, Muang, Nakorn Pathom 73000, Thailand

² Department of Chemical Engineering, College of Engineering, Rangsit University, Muang, Pathumthani 12000, Thailand

* Correspondence: wanvimon@rsu.ac.th

Abstract: Liquid natural rubber (LNR), a depolymerized natural rubber (NR) consisting of shorter chains, was prepared via oxidative degradation using NaNO_2 and H_2O_2 degrading agents in the presence of HCOOH . The influence of reagent concentrations, temperature, and reaction time on the number-average molecular weight (M_n) was studied. Results showed the higher concentration of H_2O_2 and HCOOH employed faster degradative rates. However, a higher concentration of NaNO_2 decreased the M_n reduction. Prolonged reaction time and high temperature resulted in a product with low M_n . FTIR spectra indicated the synthesized LNR contained hydroxyl end groups resulting from the breaking of the NR chains at an acidic pH, whereas a carboxyl terminated LNR was formed at an alkaline pH. SEM micrographs showed the latex particles of LNR were spherical and smaller compared to NR. The experimental results showed the reaction orders of $[\text{H}_2\text{O}_2]$, $[\text{HCOOH}]$, and $[\text{NaNO}_2]$ were 1.58, 0.79, and -0.65 , respectively. In addition, the pre-exponential factor and activation energy were $1.04 \times 10^9 \text{ M}^{-1.72} \text{ t}^{-1}$ and 78.66 kJ/mol , respectively. Based on TGA analysis, the thermal stability of the rubber depended on its M_n . The LNR containing functional end groups exhibited thermal instability and could be a starting material for many applications.

Keywords: liquid natural rubber; degradation; thermal stability



Citation: Wisetkhamchai, K.;

Patthaveekongka, W.; Arayapranee, W. Study on Degradation of Natural Rubber Latex Using Hydrogen Peroxide and Sodium Nitrite in the Presence of Formic Acid. *Polymers* **2023**, *15*, 1031. <https://doi.org/10.3390/polym15041031>

Received: 6 January 2023

Revised: 14 February 2023

Accepted: 14 February 2023

Published: 19 February 2023



Copyright: © 2023 by the authors. Licensee MDPI, Basel, Switzerland. This article is an open access article distributed under the terms and conditions of the Creative Commons Attribution (CC BY) license (<https://creativecommons.org/licenses/by/4.0/>).

1. Introduction

Natural rubber (NR) is an important renewable biopolymer in many industries due to its elastic property and excellent mechanical strength. NR latex is known as a diene rubber in its repeating units of cis-1,4-isoprene, with the molecular weight varying greatly, from only a few hundred thousand to more than one million [1]. The NR can be degraded to liquid natural rubber (LNR), which has a similar microstructure to NR and consists of shorter polymeric chains and lower molecular weight ($M_w < 10^5$) [2]. It becomes a modified NR, allowing greater flexibility in the production of the NR used. LNR produced from the degradation of NR latex is related to breaking the NR chain either by direct scission of the carbon-carbon single or carbon-carbon double bonds of the polyisoprene backbone. The molecular weight of NR can be reduced by different methods such as mechanical, chemical, photochemical, ozonolysis, or thermal degradation in a dry, solution, or latex state. Mechanical degradation of NR through mastication in the air at high temperatures is usually done before processing to facilitate easy processing or incorporation of other chemicals [3]. Ibrahim et al. [4] prepared the degraded NR latex under UV light in the presence of H_2O_2 and nano TiO_2 , which was prepared via the sol-gel method. The NR chains were attacked by radicals at carbon-carbon single bond or oxidation at carbon-carbon double bond by oxygen species. LNR containing hydroxyl and carbonyl end groups was observed, resulting from chain breaking. Sillapasuwat et al. [5] synthesized the deproteinized LNR with hydroxyl end groups by the photochemical reaction. This reaction was carried out through photocatalytic decomposition of H_2O_2 when exposed to

UV light, with or without a TiO₂ film mounted on the quartz substrate. LNR was used as a compatibilizer in NR/LLDPE (linear low-density polyethylene) blends [6–8]. Dahlan et al. [6] observed the effects of various molecular weights of LNR as a compatibilizer on the physical properties of NR/LLDPE blends. The ultraviolet irradiation technique was used to prepare LNR. Adding LNR to the blends improved the interaction between the phase of the blends, and they concluded that the LNR content added to the blends marginally affected the physical properties of NR/LLDPE blends. Moreover, LNR with a molecular weight below 20,000 g/mol is an attractive material for enhancement of further modifications. The potential application of LNR with functional end groups is used as a precursor for new material. The authors of [9–11] prepared flexible foam from poly(ϵ -caprolactone) diol (PCL) and hydroxyl telechelic NR (HTNR). First, carbonyl telechelic NR (CTNR) was prepared by an oxidative chain cleavage reaction in tetrahydrofuran with periodic acid. After that, sodium borohydride was then used to change the LNR with carbonyl end group (CTNR) into LNR with hydroxyl end group (HTNR). They claimed that HTNR-based polyurethane foams had improved elastic properties and low-temperature flexibility compared to foam based on commercial polyol. LNR with a carboxyl termination and its subsequent application in NBR compounds as a reactive polymeric plasticizer was described by Dileep et al. [12]. They found that during sulfur vulcanization, the natural rubber component of the carboxyl terminated LNR attacked the NBR. Consequently, this plasticizer was neither volatile nor extractable. Nor and Ebdon [13] studied the use of gel permeation chromatography (GPC) and Fourier transform infrared (FTIR) spectroscopy to follow the kinetics of chain scission and major changes in functional groups of NR during ozonolysis in chloroform at 0 °C. They reported that the introduction of a variety of oxygenated functional groups accompanied the reduction in molecular weight of NR during ozonolysis. Many investigations concentrated on LNR [14–16] and deproteinized LNR (LDNR) [17] via oxidatively degraded using H₂O₂ and NaNO₂ reagents. The broken chains had different end groups depending on the pH of the reaction medium. Bac et al. [14] studied the in situ epoxidation of natural rubber latex in chain-scissoring conditions. The epoxide ring underwent a ring-opening process at low pH and prolonged time, forming hydroxyl, carbonyl, and ether groups. Isa et al. [15] investigated the degradation of NR using peroxide acid in the presence of NaNO₂. They found that NR depolymerized into LNR with an epoxy and a hydroxyl group. The rate of degradation was affected by reaction temperature and time. Ibrahim et al. [16] proposed the degradation mechanisms were different as H₂O₂ and NaNO₂ underwent different routes in acidic and alkaline media. The end groups of the LNR samples performed in acidic and alkaline media were found to be hydroxyl and carbonyl, respectively. Fadhillah et al. [18] studied LNR production and the effect of CoCl₂ catalyst and NaNO₂ levels on the molecular weight of LNR. They concluded that reaction time and NaNO₂ and CoCl₂ concentrations affected the molecular weight of the LNR produced. Phetphaisit and Phinyocheep [19] investigated the kinetics of degradation of NR using a combination of potassium persulfate (K₂S₂O₈) as a radical initiator and propanal as a secondary reagent. They reported that the intrinsic viscosity [η] of the LNR obtained depended on the initiator concentration, amount of propanol, dry rubber content, reaction time, and temperature. The degradation rate exhibited a second-order rate law dependence on the cleavage of a single carbon–carbon bond of a polyisoprene chain. The activation energy of the degradation reaction was 76.56 kJ/mol.

Many relevant investigations, including the effects of various chemicals and environmental conditions as well as the mechanism of NR degradation in acidic and basic environments, have been previously carried out. However, rarely have studies on the rate of NR degradation been reported. The objectives of this research were to prepare liquid natural rubber with oxidative degradation by using hydrogen peroxide (H₂O₂), formic acid (HCOOH), and sodium nitrite (NaNO₂) as reagents. Intrinsic viscosity ([η]) was characterized by the dilution method using an Ubbelohde capillary viscometer at 30 °C when toluene has operated as a solvent. The number-average molecular weight of LNR was calculated by using Mark–Houwink equation [20]. The efficiency of the degradation

of NR was determined by measuring its number-average molecular weight (M_n). The effects of reaction parameters such as H_2O_2 , $HCOOH$, and $NaNO_2$ concentrations, reaction temperature, and reaction time were investigated. The LNR was then characterized for its chemical structure using FTIR, while scanning electron microscopy (SEM) was used to observe the morphology of the latex particles. The degradative kinetics of the NR to form LNR based on molecular weight data have been evaluated. The thermal decomposition of the rubber samples was studied in terms of thermogravimetric analysis (TGA) and derivative thermogravimetric (DTG).

2. Materials and Methods

2.1. Materials

High ammonia natural rubber latex (60% dry rubber content) used in the present study was purchased from Bothong Natural Rubber Trade Co., Ltd., Bothong, Chonburi, Thailand. 50 wt% aqueous hydrogen peroxide (H_2O_2), 85 wt% formic acid ($HCOOH$), 97 wt% sodium nitrite ($NaNO_2$), and 98 wt% sodium sulfite (Na_2SO_3) were purchased from Sigma-Aldrich, Missouri, USA. Polyoxyethylene styrenated phenyl ether ($C_{24}H_{22}O_2$) used as a surfactant under the trade name Emulvin WA was purchased from Chemical and Materials Co., Ltd., Map Pong, Chom Thong, Bangkok, Thailand. Methanol (commercial grade) was bought from Facobis Co., Ltd. (Bangkok, Thailand). All chemical reagents were used as received. Distilled water was used throughout the work.

2.2. Degradation of Natural Rubber Latex

A total of 227 g of the NR latex, having 60% DRC, was mixed with Emulvin WA and distilled water in a flask equipped with a condenser and stirrer. The NR latex was acidified by formic acid to the required pH followed by successive treatment with 50% aqueous H_2O_2 and 10% solution of $NaNO_2$. The reaction mixture was diluted to 1 L with distilled water and kept in latex form at a constant temperature for desired time. After the reaction, 5% sodium sulfite solution was added to the mixture to remove excess H_2O_2 [21], followed by precipitation with methanol. Then precipitated LNR was washed two times with distilled water and dried in a vacuum oven at 40 °C until a constant weight was achieved.

2.3. Characterization

2.3.1. Number-Average Molecular Weights

The rubber was further purified by dissolving it in toluene at room temperature for 24 h. After the sample had been dissolved, the solution was transferred by passing through a cotton filter and re-coagulated into methanol. The coagulated rubber product was washed three times with distilled water and then dried to a constant weight in a vacuum oven at 40 °C.

Viscometry, a popular method used to determine molecular weight, is quick and simple and requires a relatively inexpensive apparatus. According to ASTM D445, the Ubbelohde viscometer was used to determine the intrinsic viscosities of the rubber samples in toluene at 30 °C by extrapolation to zero concentrations of specific viscosity measurements at five different concentrations.

The average molecular weights of the rubber samples were determined by gel permeation chromatography (GPC, Alliance, Waters e2695 separations, Milford, MA, USA.) using tetrahydrofuran (THF) as eluent and polystyrene for standard calibration at 30 °C. The rubber sample was dissolved in THF and filtered using a 0.45 μm syringe filter before injecting it into a chromatograph.

Based on the Mark–Houwink equation, the relationship between the intrinsic viscosity and average molecular weight was built for the rubber sample in toluene at 30 °C. The slice log molecular weight curve of LNR samples with different intrinsic viscosities is shown in Figure 1. The relationship between number-average molecular weight (M_n) and $[\eta]$ can be described as Equation (1):

$$[\eta] = KM_n^a \quad (1)$$

where K and a are constants for a certain solvent and temperature. Figure 2 shows the plot of $\log [\eta]$ versus $\log M_n$ for rubber samples, which yielded a straight line, and the values of a and K were obtained from the slope and the intercept of this line, respectively. These K and a values of the Mark–Houwink equation were further used to transform the $[\eta]$ of the rubber sample into M_n . Then the following Equation (2) was obtained:

$$[\eta] = 1.307 \times 10^{-3} M_n^{0.638} \tag{2}$$

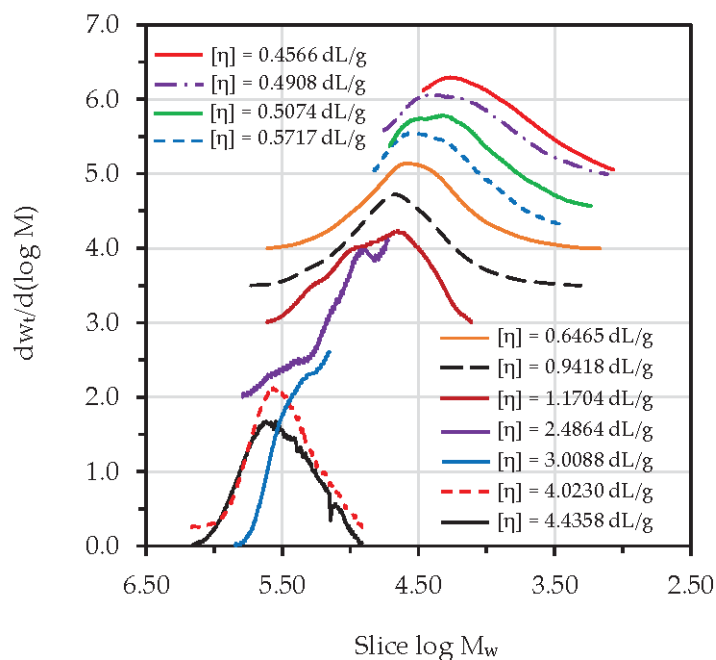


Figure 1. Molecular weight distribution curves from GPC experiments of rubber samples.

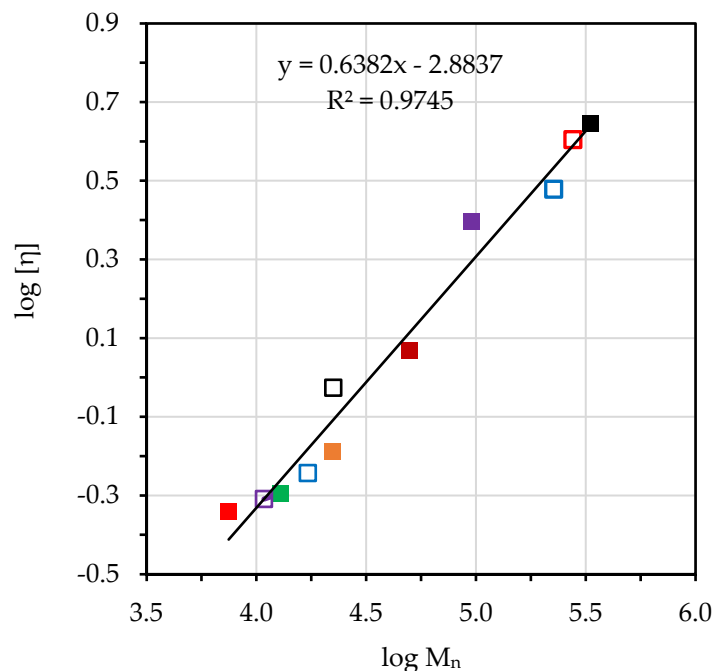


Figure 2. Relation of $\log [\eta]$ and $\log M_n$ for rubber samples in toluene at 30 °C.

2.3.2. FTIR Spectroscopy

The chemical structure of rubber samples was determined by attenuated total reflectance-Fourier-transform infrared (ATR-FTIR) spectroscopy (Perkin Elmer Frontier, CT, USA.). The samples were analyzed in transmittance mode within the range 600–4000 cm^{-1} .

2.3.3. Morphology

The morphology of rubber particles was analyzed using a field emission-scanning electron microscope (FE-SEM, Tescan, Mira3, Brno, Czech Republic.). Samples were coated with the thin gold layer and detected by backscattered electrons with an acceleration of 5 kV.

2.3.4. Thermal Analysis

The thermal degradation of rubber samples was carried out by a thermogravimetric analyzer (TGA, Perkin Elmer, Pyris 1, CT, USA.). The sample was weighted to 5.0 ± 0.2 mg in alumina crucibles. TGA was conducted from ambient to 800 $^{\circ}\text{C}$ at a heating rate of 40 $^{\circ}\text{C}/\text{min}$ under an air flow at 20 mL/min. Continuous recordings of the rubber sample's temperature, mass, and heat flow were performed.

3. Results and Discussion

3.1. FTIR Spectroscopy

Infrared spectra of the NR starting material and the obtained LNRs at various pH were compared, as shown in Figure 3. The obtained LNR exhibited the absorption peaks of C=C stretching and =C-H bending at 1665 and 834 cm^{-1} , similar to those observed in the NR. The FTIR spectra of LNR samples prepared at different pH showed a few new peaks compared to the NR. For the LNR sample prepared in an acid medium, a broad peak located at 3400 cm^{-1} was assigned for the stretching mode of the hydroxyl groups of LNR chains. Meanwhile, the presence of other groups on the LNR chains prepared in neutral and alkaline media can be attributed to the appearance of carbonyl peaks (C=O) at 1720 cm^{-1} for ketone and 1739 cm^{-1} for aldehyde, respectively.

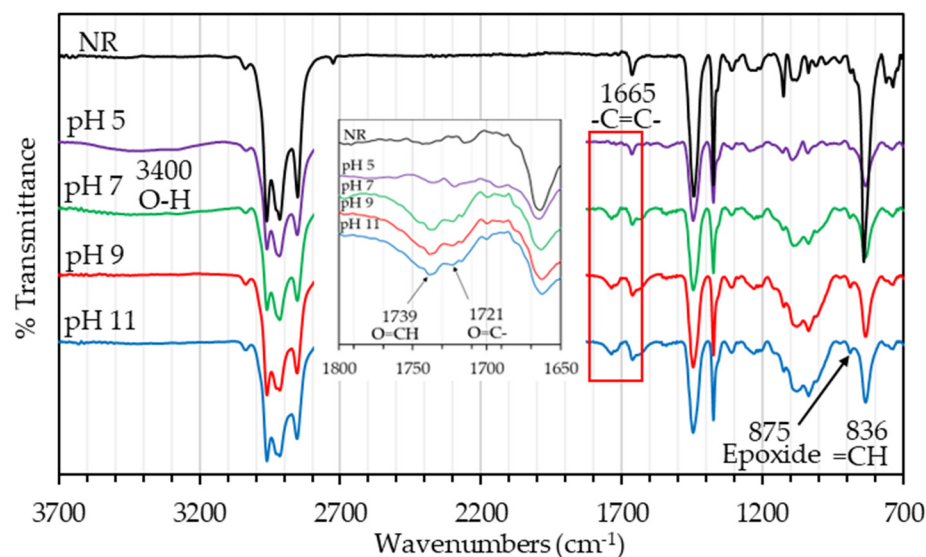


Figure 3. FTIR spectra of LNR samples prepared at different pHs using 0.4 M H_2O_2 and 0.02 M NaNO_2 at 65 $^{\circ}\text{C}$ for 12 h.

The chain breaking of NR at the carbon–carbon single bond is usually due to an attack of radicals and leaving a hydroxyl end group. In contrast, an oxidizing agent can oxidize the broken carbon–carbon double bond in the NR chains to leave a carbonyl end group. Mechanisms of LNR samples prepared via oxidative degradation using NaNO_2 and H_2O_2 reagents were found to have different end groups, hydroxyl, and carbonyl, depending

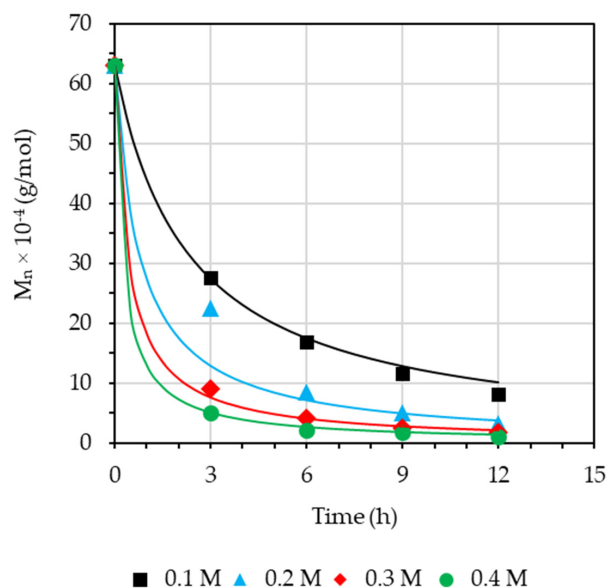


Figure 4. The effect of the concentration of H₂O₂ on M_n of LNR (filled symbols) at different reaction times. The line is the kinetic model.

Condition: pH = 5, NaNO₂ = 0.02 M, and T = 338 K.

3.3. Effect of Concentration of Formic Acid

The amount of formic acid used was adjusted to the required pH (pH 5–11). We studied the influence of HCOOH concentration on the M_n at various reaction times over the range of approximately 0.0187 M (pH 11) to 0.1247 M (pH 5) while keeping the [H₂O₂], [NaNO₂], and temperature constant, as shown in Figure 5. A higher concentration of HCOOH provided more sources of hydrogen ions, hence increasing the amount of peroxyxynitrite acid releasing •OH and •NO₂ radicals. Consequently, an increase in HCOOH concentration also increased the rate of degradation of LNR. Based on Figure 5, the degradation of NR at an acidic pH showed to be more effective than at an alkaline pH, thus yielding LNR with lower M_n.

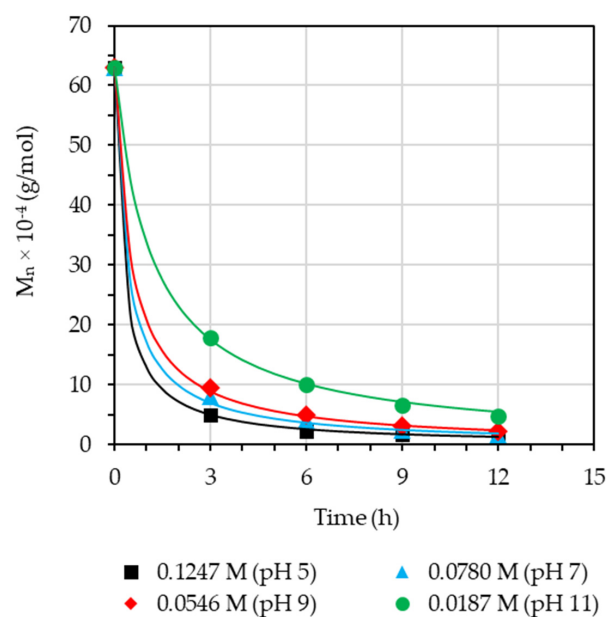


Figure 5. The effect of the concentration of HCOOH on M_n of LNR (filled symbols) at different reaction times. The line is the kinetic model.

Condition: $\text{H}_2\text{O}_2 = 0.4 \text{ M}$, $\text{NaNO}_2 = 0.02 \text{ M}$, and $T = 338 \text{ K}$.

3.4. Effect of Concentration of Sodium Nitrite

The effect of the concentration of NaNO_2 on the number-average molecular weight at various reaction times was studied over the range of approximately 0.02 to 0.2 M while keeping the $[\text{H}_2\text{O}_2]$, pH, and temperature constant, as shown in Figure 6. The results showed that an increasing concentration of NaNO_2 increased the M_n of LNR at the same reaction time. The increase in M_n was due to the higher concentration of nitrite ions, which can be oxidized by the $\bullet\text{OH}$ radicals, providing an excessive amount of $\bullet\text{NO}_2$ radicals and hydroxide (OH^-). The $\bullet\text{NO}_2$ radicals became exceedingly unstable in an aqueous solution [22,23], so it coupled with itself to form N_2O_4 , and hydrolysis of N_2O_4 in water generated HNO_2 . The HNO_2 reacted with $\bullet\text{OH}$ to produce $\bullet\text{NO}_2$. The formation of side reactions led to the reduction of $\bullet\text{OH}$ radicals that inhibited degradative reaction or triggered crosslinking reaction at higher NaNO_2 concentrations [24].

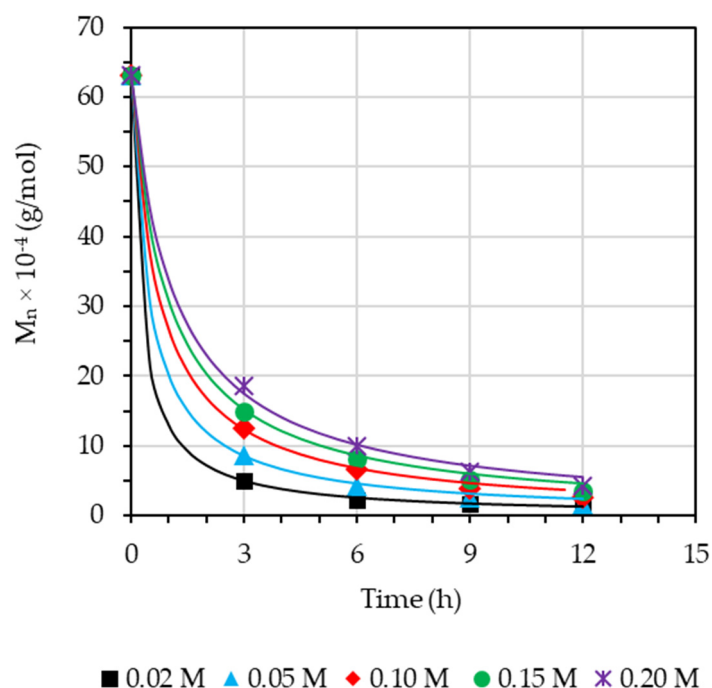


Figure 6. The effect of the concentration of NaNO_2 on M_n of LNR (filled symbols) at different reaction times. The line is the kinetic model.

Condition: $\text{H}_2\text{O}_2 = 0.4 \text{ M}$, $\text{pH} = 5$, and $T = 338 \text{ K}$.

3.5. Effect of Reaction Temperature

The effect of the temperature degradation on molecular weight was performed at 328, 333, 338, and 343 K for various reaction times by fixing the concentration of other reagents, as shown in Figure 7. The temperature influenced the efficiency of the degradation reaction. Higher reaction temperatures provided more energy to excite the molecules and allowed many chain-scissoring reactions to occur faster. Thus, an increase in reaction temperature also increased the rate of degradation of NR.

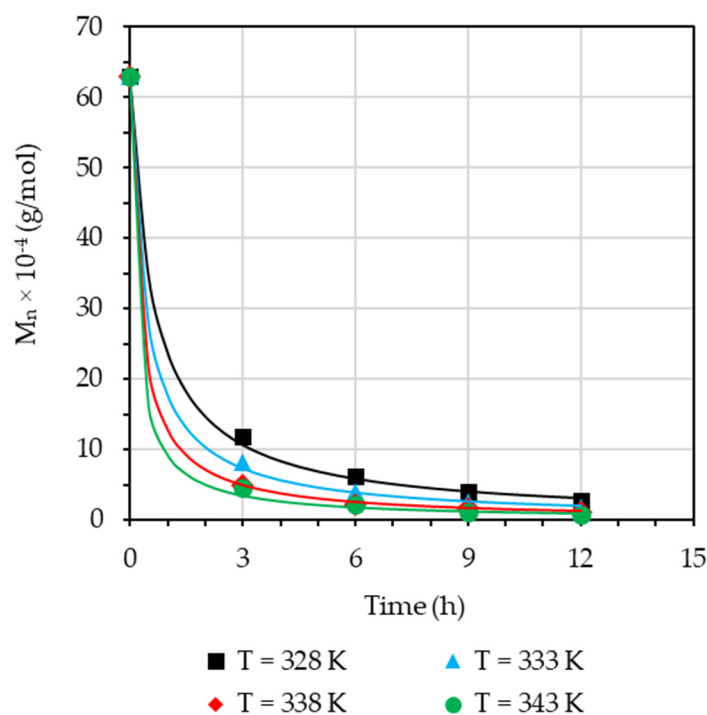


Figure 7. The effect of reaction temperature on M_n of LNR (filled symbols) at different reaction times. The line is the kinetic model.

Condition: $H_2O_2 = 0.4$ M, $pH = 5$, $NaNO_2 = 0.02$ M.

3.6. Effect of Reaction Time

The effect of reaction time on M_n of LNR was investigated by varying the reaction time from 3 to 12 h. It can be noticed that the M_n values of all rubber samples were exponentially reduced according to the increased reaction time, as shown in Figures 4–7. With an increase in reaction time, the M_n values in all cases tended to decrease significantly during the first 3 h and then decreased after 3 h of reaction time. There was a gradual decrease in the M_n when the reaction time was extended to 9 and 12 h. The morphology of NR and LNR particles at different molecular weights was investigated with an SEM micrograph, as shown in Figure 8a–d. There was much difference in the case of latex particle morphology. The spherical and pear shape had the biggest sizes before the oxidative degradation, as shown in Figure 8a. According to the above-mentioned factors, prolonged reaction times allowed more degradation of rubber chains into smaller particles. It was found that some of the latex particles were spherical, smaller, and had a wider size range compared to the NR particles after 3 h of degradative reaction (Figure 8b). After 12 h of degradation, Figure 8d shows that the latex particles were almost uniform and the smallest in size.

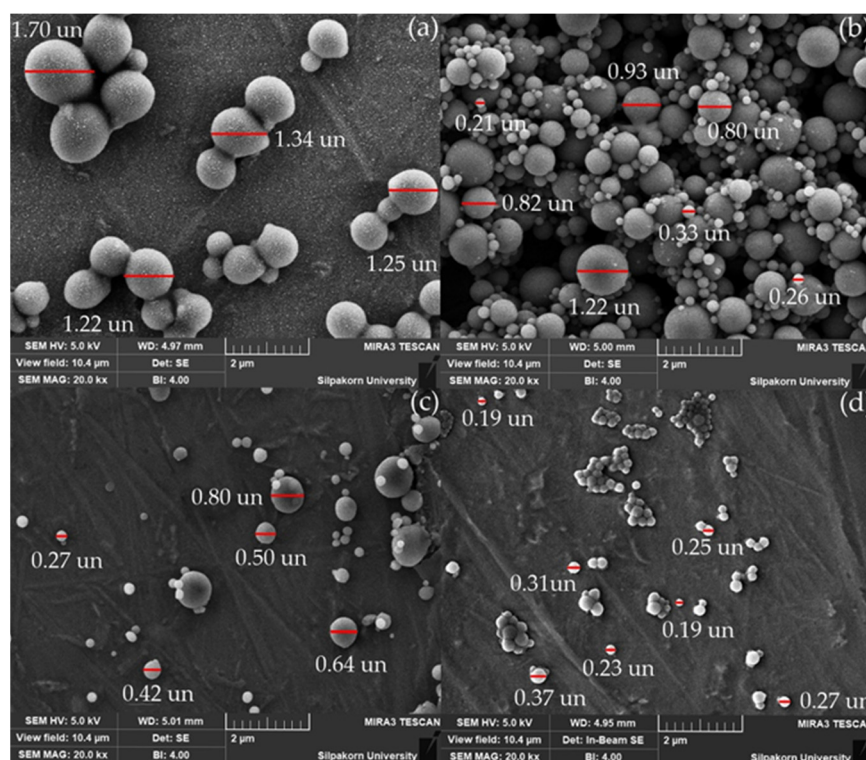


Figure 8. SEM micrographs (20,000 \times) of the rubber particles after degradation at different reaction times: (a) NR, (b) 3 h, (c) 6 h, and (d) 12 h. (The red line is diameter).

Condition: $\text{H}_2\text{O}_2 = 0.4 \text{ M}$, $\text{pH} = 5$, $\text{NaNO}_2 = 0.02 \text{ M}$, and $T = 338 \text{ K}$.

3.7. Degradative Kinetics

The degradative reaction of the LNR chains can be determined as a second-order reaction with respect to the number of bonds broken during depolymerization [25–27]. Referring to Equation (2), the intrinsic viscosity obtained can be calculated to the M_n values. A chain scission model for random scission of the macromolecule can be derived as in Equation (3):

$$\frac{1}{M_{n(t)}} - \frac{1}{M_{n(0)}} = \frac{kt}{M_0} \quad (3)$$

where $M_{n(t)}$ is the M_n of LNR at time = t , $M_{n(0)}$ is the M_n of NR at time = 0, M_0 is the M_n of isoprene unit (68 g/mol), and k is the rate constant. As previously discussed, process parameters, i.e., H_2O_2 concentration, HCOOH concentration, NaNO_2 concentration, and temperature, significantly influence the degradation process. According to the Arrhenius relation, $k = A \times \text{Exp}(-E_a/RT)$ where A , E_a , R , and T are the pre-exponential factor, activation energy, gas constant, and temperature, respectively. These parameters have been proposed to relate to the kinetic model as a power function. Therefore, Equation (3) can be rewritten as Equation (4):

$$\frac{M_0}{M_{n(t)}} - \frac{M_0}{M_{n(0)}} = A \times e^{-\frac{E_a}{RT}} [\text{H}_2\text{O}_2]^m [\text{CH}_2\text{O}_2]^n [\text{NaNO}_2]^o \times t \quad (4)$$

where $[\text{H}_2\text{O}_2]$, $[\text{HCOOH}]$, and $[\text{NaNO}_2]$ are the initial concentration of reagents (mol/L). The exponents of the reactant concentrations m , n , and o are referred to as partial orders of the reaction that must be determined experimentally. The partial order corresponding to each reactant is now calculated by conducting the reaction with varying concentrations of the reactant in question, and the concentrations of the other reactants are kept constant.

Generally, the kinetic model, a power function of the process variables, is independent of time. Referring to Figures 4–6, the partial orders can be determined by using a log $[(M_0/M_{n(t)} - M_0/M_{n(0)})/t]$ -log [reactant] plots and the linear regression technique, as shown in Figures 9–11. The corresponding slopes were the partial orders given by m , n , and o , respectively.

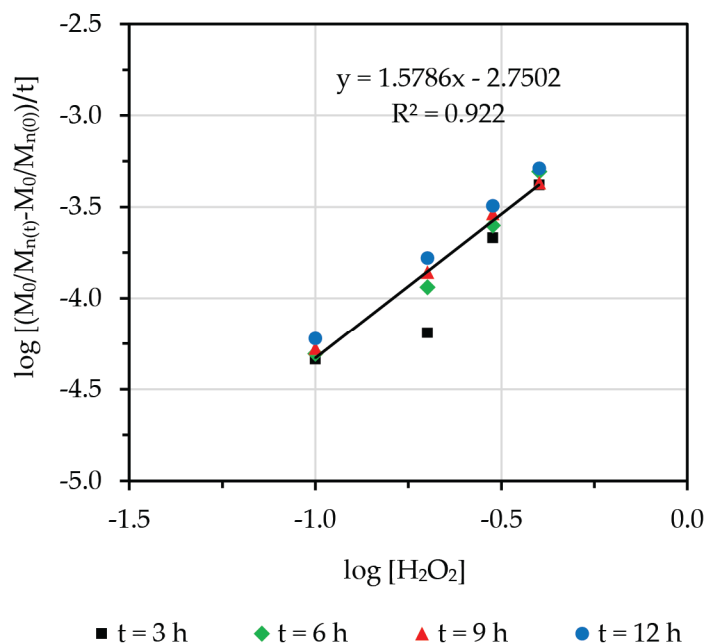


Figure 9. A log-log plot of $[(M_0/M_{n(t)} - M_0/M_{n(0)})/t]$ versus H_2O_2 concentration at different reaction times.

Condition: pH = 5, $NaNO_2 = 0.02$ M, and $T = 338$ K.

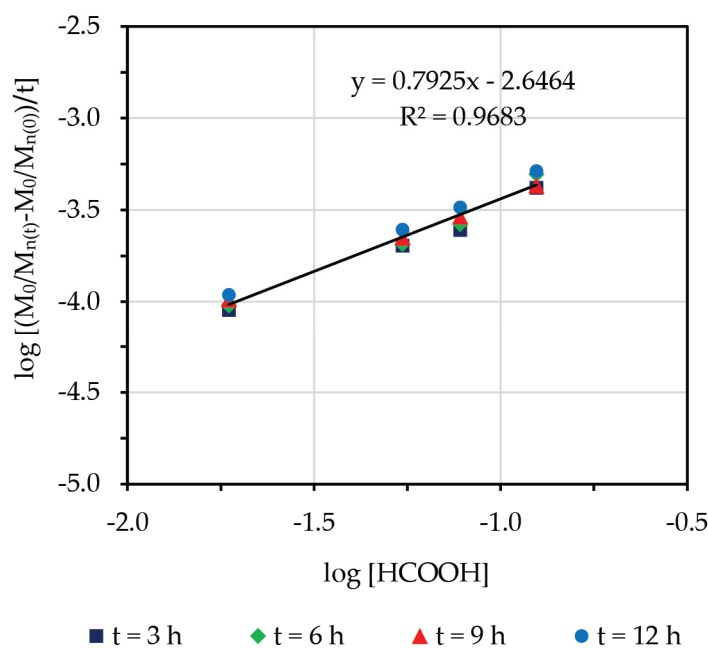


Figure 10. A log-log plot of $[(M_0/M_{n(t)} - M_0/M_{n(0)})/t]$ versus HCOOH concentration at different reaction times.

Condition: $H_2O_2 = 0.4$ M, $NaNO_2 = 0.02$ M, and $T = 338$ K.

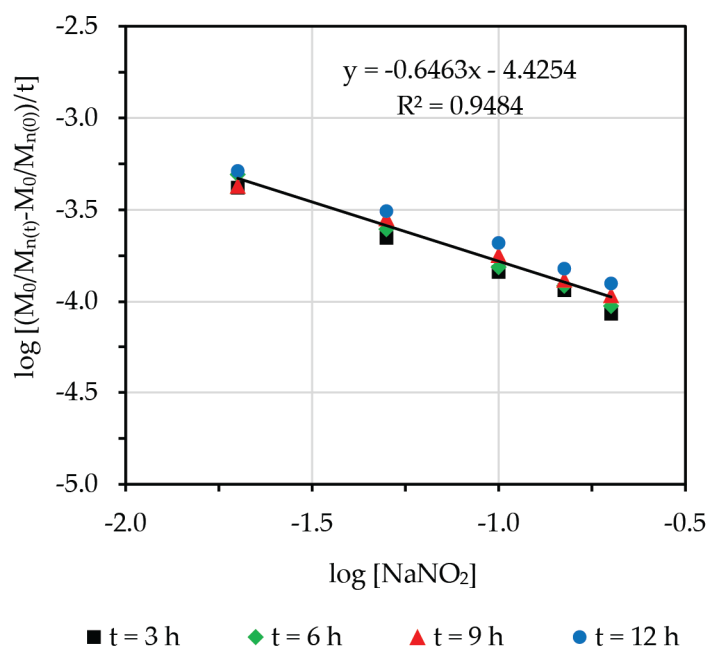


Figure 11. A log-log plot of $[(M_0/M_{n(t)} - M_0/M_{n(0)})/t]$ versus NaNO_2 concentration at different reaction times.

Condition: $\text{H}_2\text{O}_2 = 0.4 \text{ M}$, $\text{pH} = 5$, and $T = 338 \text{ K}$.

Referring to Figure 7, a plot of $\ln [(M_0/M_{n(t)} - M_0/M_{n(0)})/([0.4]^{1.58}[0.1247]^{0.79}[0.02]^{-0.65} \times t)]$ versus $1000/T$ gave a straight line whose slope is equal to $-1000E_a/R$ and whose intercept with the y axis is $\ln A$, as shown in Figure 12.

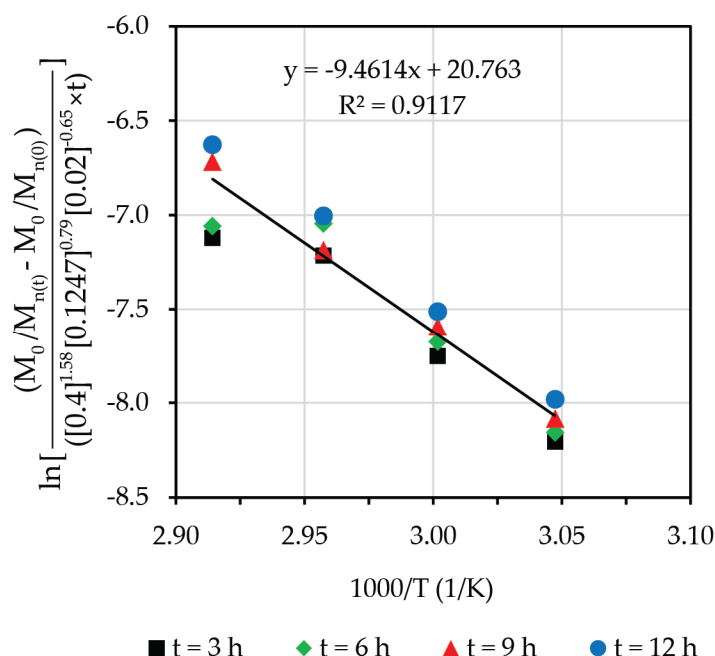


Figure 12. A natural logarithm plot of $[(M_0/M_{n(t)} - M_0/M_{n(0)})/([0.4]^{1.58}[0.1247]^{0.79}[0.02]^{-0.65} \times t)]$ versus $1000/T$ at different reaction times.

Condition: $\text{H}_2\text{O}_2 = 0.4 \text{ M}$, $\text{pH} = 5$, and $\text{NaNO}_2 = 0.02 \text{ M}$.

The reaction orders with respect to H_2O_2 concentration and HCOOH concentration deviated from 1, indicating a nonlinear relationship between the degradative reaction. An increase in reaction temperature and the concentrations of H_2O_2 and HCOOH enhanced the

chain-scissoring reaction. On the other hand, the negative power of NaNO_2 concentration indicated that the M_n reduction was inversely proportional to NaNO_2 concentration. Hence, an increase in NaNO_2 concentration retarded the depolymerization rate. The reaction orders of $[\text{H}_2\text{O}_2]$, $[\text{HCOOH}]$, and $[\text{NaNO}_2]$ were 1.58, 0.79, and -0.65 , respectively (Figures 9–11). According to Figure 12, The pre-exponential factor and activation energy were found to be $1.04 \times 10^9 \text{ M}^{-1.72} \text{ t}^{-1}$ and 78.66 kJ/mol , respectively, according to Figure 12. As a result, the kinetic model for random scission of NR using H_2O_2 , HCOOH , and NaNO_2 as reagents can be summarized as Equation (5):

$$\frac{M_0}{M_{n(t)}} - \frac{M_0}{M_{n(0)}} = 1.04 \times 10^9 \text{ M}^{-1.72} \text{ t}^{-1} e^{\frac{-78.66 \cdot \text{kJ} \cdot \text{mol}^{-1}}{RT}} [\text{H}_2\text{O}_2]^{1.58} [\text{CH}_2\text{O}_2]^{0.79} [\text{NaNO}_2]^{-0.65} \times t \quad (5)$$

Figure 13 shows a satisfactory relationship between the experimental and predicted values obtained from Equation (5) of degradation of NR. The kinetic parameters were estimated based on experimental data. When R^2 was equal to 0.9771, the data prediction showed good performance and a high correlation between the predicted value obtained from Equation (5) and the experimental value.

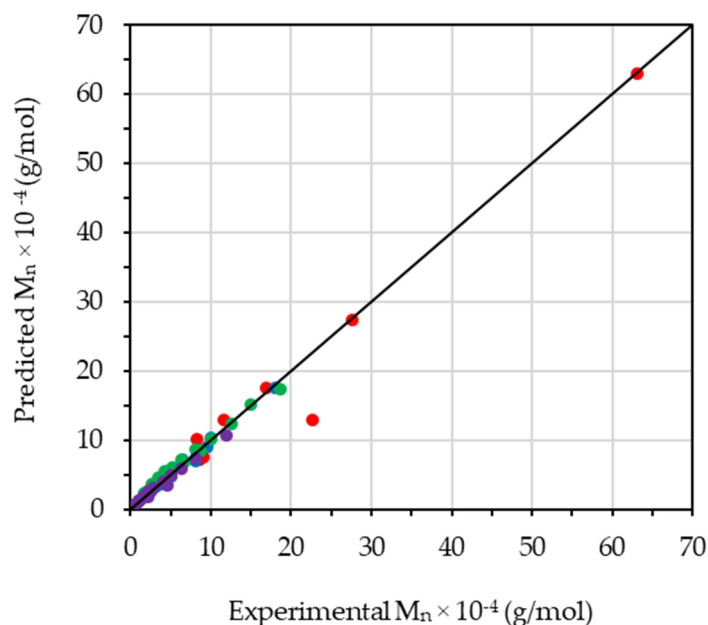


Figure 13. Correlation between the predicted values obtained from Equation (5) and experimental data with $R^2 = 0.9771$.

3.8. TGA Analysis

The curves of NR and LNR samples in the air atmosphere were investigated by a thermogravimetric analysis (TGA) instrument, which described the decomposition behavior of NR and LNR at different number-average molecular weights, as shown in Figure 14. Referring to Figure 14a, thermogravimetric (TG) curves are weight loss against temperature at a heating rate of $40 \text{ }^\circ\text{C/min}$. The decomposition of NR and LNR samples occurred one step in the temperature range of $50\text{--}850 \text{ }^\circ\text{C}$. The thermal degradation temperatures of NR and LNR at different molecular weights are listed in Table 1. The initial decomposition temperature (T_i) and final decomposition temperature (T_f) using a bitangent method were obtained TGA curve, and temperature at maximum weight loss rate (T_m), which can be obtained from the peak of the DTG curves, as shown in Figure 14b. It can be seen that the thermal degradation temperature of LNR samples decreased with a decrease in the M_n . NR had a T_i , T_m , and T_f of $392 \text{ }^\circ\text{C}$, $429 \text{ }^\circ\text{C}$, and $469 \text{ }^\circ\text{C}$, respectively, while all LNRs exhibited lower degradation temperatures when compared with NR. The T_m of LNR decreased from $428 \text{ }^\circ\text{C}$ to $398 \text{ }^\circ\text{C}$ when the M_n decreased from $50,023$ to $10,825 \text{ g/mol}$. The thermal

degradation curves of LNR, compared to NR, shifted to lower temperatures. This shows that the reduction in molecular weight led to thermal instability resulting in a reactive material, which can be more prone to reacting with lower energy usage.

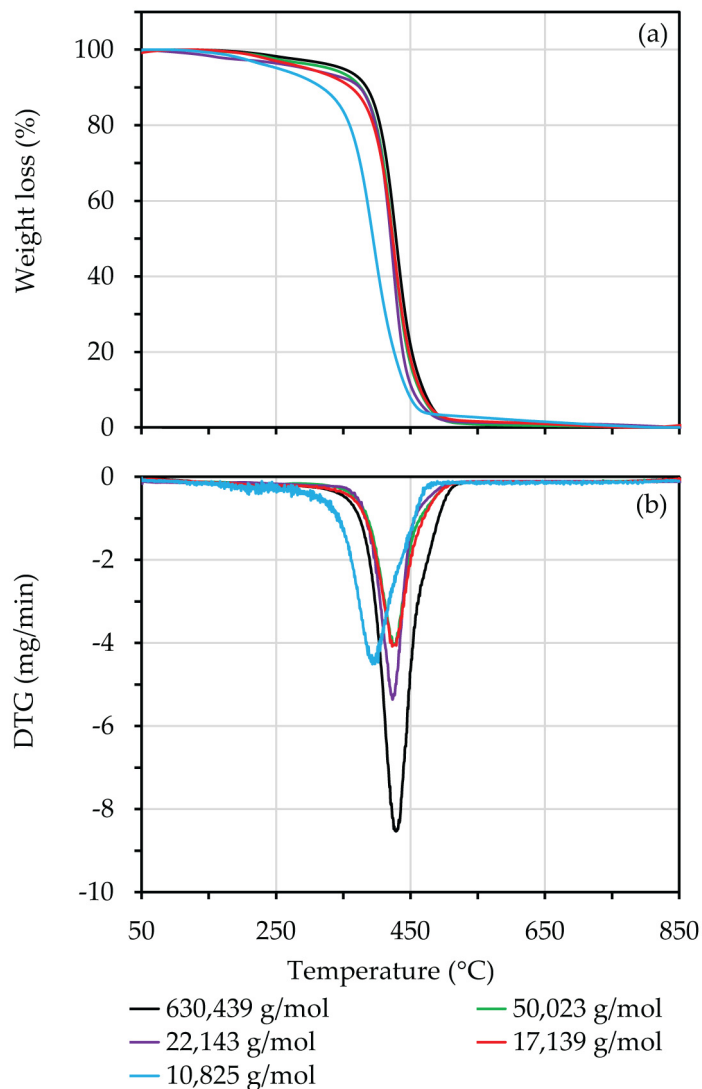


Figure 14. TGA (a) and DTG (b) thermograms of NR and LNR at different molecular weights at 40 °C/min.

Table 1. T_i , T_m , and T_f of NR and LNR at different molecular weights.

M_n (g/mol)	Heating Rate = 40 °C/min		
	T_i (°C)	T_m (°C)	T_f (°C)
630,439	392	429	469
50,023	388	428	468
22,143	380	424	466
17,139	375	419	461
10,825	352	398	439

4. Conclusions

Natural rubber (NR), which has a molecular weight of a few hundred thousand to more than one million, is found in the form of latex. The natural rubber depolymerization process used NaNO_2 and H_2O_2 degrading agents in the presence of HCOOH to produce

liquid natural rubber (LNR) with a relatively low molecular weight. This study resulted in the Mark–Houwink equation for the value of the constant K , and a for NR and LNR samples were 1.307×10^{-3} and 0.638 respectively, which were used to determine the number-average molecular weight. The molecular weight of LNR obtained depended on concentrations of H_2O_2 , $HCOOH$, and $NaNO_2$, temperature, and reaction time. It was found that the higher concentration of H_2O_2 and $HCOOH$ employed faster rates of degradation. However, a higher concentration of $NaNO_2$ decreased the M_n reduction. The high degradative temperature made the NR chains break more rapidly. The M_n values were a rapid initial decrease followed by a more gradual fall according to the increased reaction time. The results showed that the lowest M_n of the resulting LNR product was 10,825 g/mol from the initial molecular weight of 630,439 g/mol. Based on FTIR analysis, the presence of hydroxyl terminal groups resulting from the breaking of the NR chains was synthesized at acidic pH. In contrast, LNR with carbonyl terminal groups was formed as the degradative reaction at alkaline pH. SEM micrographs showed the NR latex particles were small spheres with a few larger pear shape particles. After the degradation process, the LNR latex obtained showed distinctly smaller spherical-shaped particles as compared to the NR particles. Changes in the molecular weight were used to construct a kinetic model for the depolymerization process: $(M_0/M_{n(t)}) - (M_0/M_{n(0)}) = [(1.04 \times 10^9 M^{-1.72} t^{-1} \text{Exp}(78.66 \text{ kJ mol}^{-1})][H_2O_2]^{1.58}[HCOOH]^{0.79}[NaNO_2]^{-0.65} t$. The kinetic model is useful to estimate the number-average molecular weight for degraded NR under different environmental conditions such as H_2O_2 , $HCOOH$, and $NaNO_2$ concentrations, reaction temperature, and reaction time. From TGA measurements, the decomposition temperatures decreased with a decrease in the M_n , indicating that the LNR had worse thermal stability than NR. Therefore, LNR should be widely used as a starting material for synthesizing biopolymers.

Author Contributions: Writing-original draft preparation, K.W.; writing-review and editing, W.P. and W.A. All authors have read and agreed to the published version of the manuscript.

Funding: This research was funded by the Thailand Research Fund (TRF) under the Royal Golden Jubilee Ph.D. Program, grant number PHD/0209/2558.

Institutional Review Board Statement: Not applicable.

Data Availability Statement: All the data is included in the article.

Acknowledgments: The authors gratefully acknowledge the financial support of the Thailand Research Fund (TRF) and Silpakorn University through the Royal Golden Jubilee Ph.D. Program grant #PHD/0209/2558.

Conflicts of Interest: The authors declare no conflict of interest.

References

1. Ibrahim, S.; Othman, N.; Ismail, H. Degradation of natural rubber latex. In *Natural Rubber: Properties, Behavior and Application*; Hamilton, J.L., Ed.; Nova Science Publishers, Inc.: Hauppauge, NY, USA, 2016; pp. 105–136.
2. Azhar, N.H.A.; Jamaluddin, N.; Md Rasid, H.; Mohd Yusof, M.J.; Yusoff, S.F.M. Studies on Hydrogenation of Liquid Natural Rubber Using Diimide. *Int. J. Polym. Sci.* **2015**, *2015*, 1–6. [[CrossRef](#)]
3. Abdullah, I. Liquid natural rubber: Preparation and application. *Prog. Polym. Sci.* **1994**, *3*, 351–365.
4. Ibrahim, S.; Othman, N.; Sreekantan, S.; Tan, K.; Mohd Nor, Z.; Ismail, H. Preparation and Characterization of Low-Molecular-Weight Natural Rubber Latex via Photodegradation Catalyzed by Nano TiO_2 . *Polymers* **2018**, *10*, 1216–1233. [[CrossRef](#)]
5. Sillapasuwana, A.; Saekhow, P.; Rojruthai, P.; Sakdapipanich, J. The Preparation of Hydroxyl-Terminated Deproteinized Natural Rubber Latex by Photochemical Reaction Utilizing Nanometric TiO_2 Depositing on Quartz Substrate as a Photocatalyst. *Polymers* **2022**, *14*, 2877–2889. [[CrossRef](#)]
6. Dahlan, H.M.; Khairul Zaman, M.D.; Ibrahim, A. Liquid natural rubber (LNR) as a compatibilizer in NR/LLDPE blends. *J. Appl. Polym. Sci.* **2000**, *78*, 1776–1782. [[CrossRef](#)]
7. Abdullah, I.; Ahmad, S.; Sulaiman, C.S. Blending of natural rubber with linear low-density polyethylene. *J. Appl. Polym. Sci.* **1995**, *58*, 1125–1133. [[CrossRef](#)]
8. Ibrahim, A. Thermoplastic natural rubber blends. *Prog. Polym. Sci.* **1998**, *23*, 665–706. [[CrossRef](#)]

9. Panwiriyarat, W.; Tanrattanakul, V.; Pilard, J.-F.; Pasetto, P.; Khaokong, C. Effect of the diisocyanate structure and the molecular weight of diols on bio-based polyurethanes. *J. Appl. Polym. Sci.* **2013**, *130*, 453–462. [[CrossRef](#)]
10. Panwiriyarat, W.; Tanrattanakul, V.; Pilard, J.-F.; Pasetto, P.; Khaokong, C. Preparation and Properties of Bio-based Polyurethane Containing Polycaprolactone and Natural Rubber. *J. Polym. Environ.* **2013**, *21*, 807–815. [[CrossRef](#)]
11. Saetung, A.; Rungvichaniwat, A.; Campistron, I.; Klinpituksa, P.; Laguerre, A.; Phinyocheep, P.; Doutres, O.; Pilard, J.-F. Preparation and physico-mechanical, thermal and acoustic properties of flexible polyurethane foams based on hydroxytelechelic natural rubber. *J. Appl. Polym. Sci.* **2010**, *117*, 828–837. [[CrossRef](#)]
12. Dileep, U.; Avirah, S.A. Studies on carboxy-terminated liquid natural rubber in NBR. *J. Appl. Polym. Sci.* **2002**, *84*, 261–267. [[CrossRef](#)]
13. Nor, H.M.; Ebdon, J.R. Ozonolysis of natural rubber in chloroform solution Part 1. A study by GPC and FTIR spectroscopy. *Polymer* **2000**, *41*, 2359–2365. [[CrossRef](#)]
14. Bac, N.V.; Terlemezyan, L.; Mihailov, M. Epoxidation of natural rubber in latex in the presence of a reducing agent. *J. Appl. Polym. Sci.* **1993**, *50*, 845–849. [[CrossRef](#)]
15. Isa, S.Z.; Yahya, R.; Hassan, A.; Tahir, M. The influence of temperature and reaction time in the degradation of natural rubber latex. *Malays. J. Anal. Sci.* **2007**, *11*, 42–47.
16. Ibrahim, S.; Daik, R.; Abdullah, I. Functionalization of Liquid Natural Rubber via Oxidative Degradation of Natural Rubber. *Polymers* **2014**, *6*, 2928–2941. [[CrossRef](#)]
17. Thuong, N.T.; Manh, N.D.; Tue, N.N. Characterization of liquid deproteinized natural rubber prepared via oxidative degradation. *Vietnam J. Chem.* **2020**, *58*, 826–831.
18. Fadhillah, I.; Wiranata, A.; Zahrina, I. Molecular Weight of Liquid Natural Rubber (LNR) Product from the Chemical Depolymerization Process of High Molecular Weight Natural Rubber Latex. *J. Phys. Conf. Ser.* **2020**, *1655*, 012091.
19. Phetphaisit, C.W.; Phinyocheep, P. Kinetics and parameters affecting degradation of purified natural rubber. *J. Appl. Polym. Sci.* **2003**, *90*, 3546–3555. [[CrossRef](#)]
20. Chen, L.; Xue, W.; Zeng, Z. Synthesis and Intrinsic Viscosity-molecular Weight Relationship of Poly(ethylene adipate). *Chem. Sci. Int. J.* **2017**, *20*, 1–9. [[CrossRef](#)]
21. Yoksan, R. Epoxidized Natural Rubber for Adhesive Applications. *Kasetsart J.* **2008**, *42*, 325–332.
22. Marussi, G.; Vione, D. Secondary Formation of Aromatic Nitroderivatives of Environmental Concern: Photonitration Processes Triggered by the Photolysis of Nitrate and Nitrite Ions in Aqueous Solution. *Molecules* **2021**, *26*, 2550. [[CrossRef](#)] [[PubMed](#)]
23. Elliot, A.J.; Simons, A.S. Reactions of NO₂ and nitrite ion with organic radicals. *Can. J. Chem.* **1984**, *62*, 1831–1834. [[CrossRef](#)]
24. Ibrahim, S.; Mustafa, A. Effect of reagents concentration and ratio on degradation of natural rubber latex in acidic medium. *Malays. J. Anal. Sci.* **2014**, *18*, 405–414.
25. Wang, Z.; Luo, W.; Li, S.; Fang, L.; Liao, S.; Li, L.; Lin, H.; He, C. Rheological Behavior of Raw Natural Rubber Coagulated by Microorganisms. *Polímeros* **2014**, *24*, 143–148. [[CrossRef](#)]
26. Elias, H.-G. *An Introduction to Polymer Science*; VCH: Weinheim, Germany, 1997; p. 166.
27. Tasakorn, P.; Amatyakul, W. Photochemical reduction of molecular weight and number of double bonds in natural rubber film. *Korean J. Chem. Eng.* **2008**, *25*, 1532–1538. [[CrossRef](#)]

Disclaimer/Publisher's Note: The statements, opinions and data contained in all publications are solely those of the individual author(s) and contributor(s) and not of MDPI and/or the editor(s). MDPI and/or the editor(s) disclaim responsibility for any injury to people or property resulting from any ideas, methods, instructions or products referred to in the content.